Appearance of Conducting Behavior in a One Dimensional Nano Resistor Identical to a Semiconductor Diode

Research Article

M. Taazeem Ansari[1], , M. Rafat[1], , A. Almohammedi[2], and M. Mudassir Husain*[1,2],

[1] Physics Section, Department of Applied Sciences and Humanities, Faculty of Engineering and Technology, Jamia Millia Islamia, New Delhi 110025, India
[2] Department of Physics, Faculty of Science, Islamic University Madinah, Madinah, Saudi Arabia
*Corresponding author: mmhusain@jmi.ac.in

Abstract. The present work deals with the simulation of electronic transport through a single dimensional carbon atoms chain device coupled to Graphene nanoribbons (GNR) electrodes. In order to observe electron transport in a more specific manner, applied voltage is regulated across an eight atoms long carbon chain resistor sandwiched between two identical semi-infinite semiconducting Armchair Graphene nanoribbon (AGNR) electrodes. The entire device is 2.06 nm in length consisting of a 0.93 nm long monoatomic carbon chain with eight carbon atoms coupled with two 1.13 nm wide 7-AGNR electrodes. Nonequilibrium green's function (NEGF) technique coupled with density functional theory (DFT) generally used to simulate electronic transport in such systems is employed. The experimental realization of stable carbon chain and 7-AGNR observed in past studies motivated us to link these two experimentally obtained carbon based materials and construct a device in order to investigate electron transport properties theoretically. Meanwhile, the continuous advancement in nanotechnology realization of such devices experimentally may be anticipated in near future, with which the authenticity of the present and other similar reported simulated results may be validated. In this device the current is calculated as a function of potential difference within the 0.0-2.5 V range. The I-V curve exhibits a nonconducting region upto 0.81 V, followed by steep rise in current magnitude to a maximum value 13.0 μA as in semiconductor diodes, involving non-linear characteristic curve displaying a sharp negative differential resistance (NDR) pattern, which is the main focus of our study. Nano devices displaying such unusual I/V characteristics have been considered for developing application oriented futuristic miniaturized devices.

Keywords. Armchair Graphene Nano Ribbons (AGNR); Monoatomic carbon chain; Non Equilibrium Greens Function (NEGF); Ballistic transport; Negative Differential Resistance (NDR); Density Functional Theory (DFT)

PACS. 85.35.-p

Received: April 8, 2020 **Accepted:** April 29, 2020

1. Introduction

Low dimensional nanosized electronic devices working on quantum mechanical principle offers promising solution to low operational power, ultrafast response time, compact, negligible heat dissipating and environment friendly diodes and transistor in the present times. Carbon based nanomaterial devices seems to be an excellent fit to fulfill all these criterion. Such miniature material devices require extremely low operational power, negligible heat dissipation due to ballistic transport mode unlike diffusive as in semiconductors, ultrafast response time and posing no threat to environment. Negative differential resistance (NDR), a special feature in the I-V characteristics in some semiconducting materials have been utilized here throughout the characteristic development of the proposed modeled functional device. In contrast to this, a large number of modeled carbon material based devices exhibiting NDR pattern in their I/V characteristics has been reported [11, 14, 17, 20, 34–36, 38, 39]. Furthermore, the development of advance experimental techniques in the field of nanoscience and technology makes such virtual research findings optimistic for construction and realization in near future. Moreover, realization of such device will surely surpass Moore's law which highlights the very aspect of size limitations in semiconducting devices that tends to converge, reaching almost saturation level due to dominance of quantum mechanical effects as size is reduced and reaches nano dimensions. Since, in the limiting dimensions the electrons particle like nature disappears and dramatically overtaken by wave nature and the entire transport paradigm based on ohms law ceases. Such proposed hypothetical devices working on quantum principle transport revolutionized electronic industry entirely in terms of generating efficient, ultra fast devices inherited with high packing density. This exceptional physical and chemical properties of carbon based material motivated us to take up the task of modeling devices out of such materials and simulate conduction behavior. Unusual conduction characteristics have been reported depending upon the, geometry and orientation of channel and electrodes. Available chemical techniques may be utilized to remove existing atom and dope it with a foreign atom which fits in the lattice site perfectly. The doped material sometimes alters the conducting characteristics drastically. In some case the magnitude of current is increased drastically and it also changes the I/V pattern.

Theoretical results reported by several groups [6, 22, 25, 30] in the past have predicted that ideal covalent bonded monoatomic carbon chain polyyne ($\cdots$C$\equiv$C$-$C$\equiv$C$\cdots$) and cumulene ($\cdots$C$=$C$=$C$=$C$\cdots$) can act as channel (resistor) of molecular devices. Earlier carbon chain has not been investigated experimentally due to lack of its production [10, 15, 31, 40]. However, Jin et al. [18] introduced a novel approach experimentally for producing stable and rigid atomic chains by detaching carbon atoms row by row from graphene sheet via electron irradiation. Jin et al. [18] then suggested that it would be very intriguing to explore the electron transport properties of a system having sp and sp^2 hybridization. In the present device, the sp hybridization exists between chain atoms and sp^2 between the C-atoms of chain and 7-AGNR electrode at the junction. The physical properties (electronic, optical and magnetic) of Graphene nanoribbon (GNRs) can be modified by changing their width and edge structures [5, 9, 19, 23, 29, 33]. Since both 1-D carbon chain and GNRs can be produced experimentally, one can expect realization of transport in a device consisting of carbon chain and AGNR electrodes

experimentally in near future. Consistency of experimental findings with simulation results will validate the importance of modeling field and provide further impetus to modeling and simulation field for investigating transport in more complex low dimensional devices.

2. Model and Method Adopted

Figure 1, shows the modeled device in order to study the electronic transport. The device in its simplest form comprises of three vital components i.e. the Left electrode (LE), the Right electrode (RE) and the scattering region (shown by dashed rectangular loop). The electrodes are semi-infinite and comprises of 7-atoms wide armchair graphene nanoribbons (7-AGNR). Each electrode consists of supercell with three repeated carbon unit cells perpendicular to the direction of electronic transport i.e. z-direction. The scattering region consists of (0.93) nm long carbon chain coupled to a super cell with two repeated carbon unit cell on either side. Modeling and calculations of the device were performed by using simulation software Atomistix Toolkit ATK/VNL [27] procured by the institute.
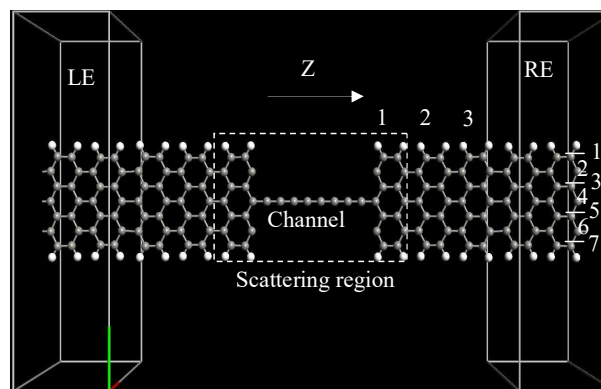

Figure 1. Schematic representation of device model used to observe transport through 8-carbon atoms, 0.93 nm long chain connected to 7-AGNR (7 carbon atoms along the width of the unit cell of AGNR) electrodes. The scattering region is enclosed in the rectangular dashed loop. The direction of electron transport is in z-direction. 1, 2, 3 shows the primitive unit cell

The transport calculations were carried out by using the Nonequilibrium green's function (NEGF) formalism [4, 7, 8, 16] and density functional theory (DFT) [12, 26]. Transport calculation through such devices is governed by the transmission function given by

$$T(E,V) = T_r[\Gamma_L(V)G^R(E,V)\Gamma_R(V)G^A(E,V)], \tag{2.1}$$

where G^R, G^A represent the retarded and advanced green's function; Γ_L and Γ_R depicts the imaginary part of left and right self-energies respectively. The I-V characteristics are analyzed by using Landauer-Büttiker formalism [2, 21] (relating transmission probability with linear conductance). The variation of current with voltage $I(V)$ depends upon the transmission function $T(E,V)$ and the bias window. The variation can be expressed by

$$I(V) = \frac{2e}{h} \int_{\mu_1}^{\mu_2} dE\, T(E,V)[f(E-\mu_L) - f(E-\mu_R)], \tag{2.2}$$

where $f(E - \mu_L/R) = \left\{ 1 + \exp\left[\frac{E - \mu_{L/R}}{k_B T} \right] \right\}^{-1}$ is the Fermi-Dirac distribution function. $\mu_L = (E_F - eV_b/2)$ and $\mu_R = (E_F + eV_b/2)$ are the electrochemical potentials of the left and right electrode and e, h are the electronic charge and Planck's constant respectively. The fermi level ε_F is set to be zero throughout the electronic transport calculations. The integrated area under the transmission curve within the bias window $(-V_b/2, V_b/2)$ where (V_b is the bias voltage) gives the magnitude of current corresponding to different applied bias. The optimization of device geometry is done within the frame of reference of Brenner empherical potential [3] such that the maximum force appearing on each atom is less than $0.001 \, \text{eV/A}^3$. A single-zetapolarized basis set is used for both carbon and hydrogen atom along with $1 \times 1 \times 100$ Monkhorst pack k-points grid to enhance the transport calculations thereby reducing the convergence time. The transmission calculations were carried out keeping electron temperature at $300\,\text{K}$ and by applying local density approximation (LDA) as exchange-correlation potential and subsequently keeping the mesh cut off at $150\,\text{Ry}$. The core-electrons are modelled in context with Troullier-Martins non-local pseudopotential [32].

3. Results and Discussion

The perfection with which the resistor is coupled with electrodes is important in determining the I-V characteristics of any electronic device. A strong coupling of channel with electrodes i.e. the interaction of channel with electrode's atoms is often desired, as it ensures perfect matching of density of states (DOS) between the two components and smooth flow of electrons from source to drain, and enhances the conducting behavior of device. Perfect coupling between dissimilar material channel and electrodes is rather difficult to achieve, due to which the conducting properties of device is adversely affected and most of the power is lost due to dissipated heat at the contacts. The coupling problem does not arise in the proposed device as the entire device (contacts and channel) can be carved out from a 2-D graphene sheet by electron radiation through advanced techniques developed and reported by Jin et al. [18] in context of carbon chain. The device that we have modeled consists of sp-hybridized eight atoms long monoatomic carbon chain of length $0.93\,\text{nm}$ coupled to three unit cells of 7-AGNR as (electrodes) with sp^2 hybridized carbon atoms. The junction displays a unique combination of sp and sp^2 hybridization. The optimized device is shown in Figure 1. The details of parameters used for stabilizing the device has been mentioned in section 2.

On applying proper biasing and regulating the voltage (with a step size of $0.5\,\text{V}$), the transmission spectrum is calculated. The calculated transmission spectrum is shown in Figure 2. The allowed and forbidden transmission at some particular value of potential can be observed by the presence and absence of transmission peaks between left and right electrochemical potential (μ) of electrodes, shown by the two slanted lines. Also, theoretically, at $0\,\text{V}$ bias, the transmission tends to zero and eqn. (2.1) can be rewritten as

$$T(E, 0) = T_r[\Gamma_L(0)G^R(E, 0)\Gamma_R(0)G^A(E, 0)]. \tag{3.1}$$

As the potential is increased, transmission peaks start appearing on either side of fermi level with in the bias window between μ_L and μ_R.
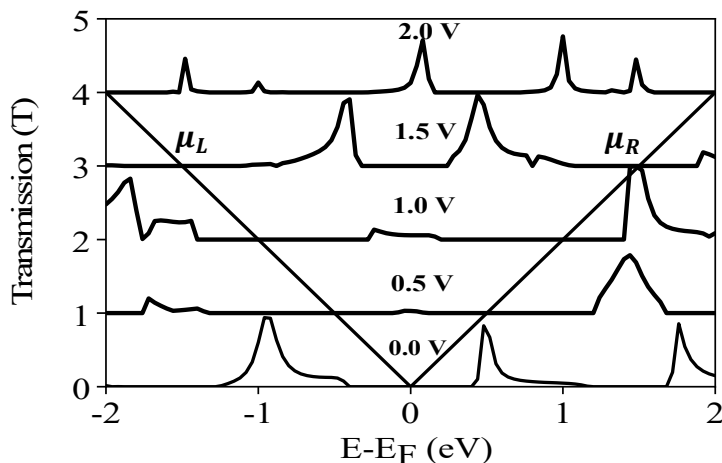
Figure 2. Transmission spectrum as a function of energy in the bias range (0-2V) with a step size of 0.5 V. The electrochemical potential μ_L and μ_R is represented by two solid slant lines. The peaks between the lines shows the possibility of transmission at that value

Figure 3 shows the partial density of states (PDOS) at applied zero bias. It can be seen from that figure that the PDOS of the chain Figure 3(a) and electrodes (b) are far away from fermi level implying zero transmission.
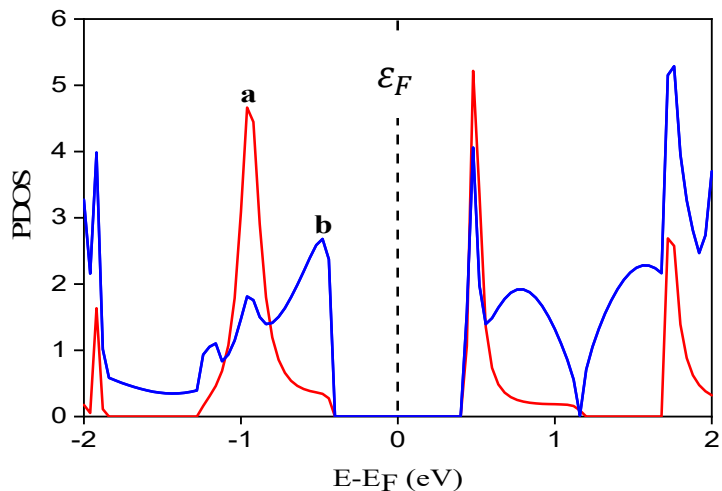

Figure 3. Partial Density of States in absence of biasing

As the potential is increased, transmission peaks start appearing on either side of fermi level with in the bias window between μ_L and μ_R. The transmission does not vary linearly with the potential difference as in ohmic conductor since the transmission is ballistic in nature for low dimensional system. The current through the device is related with transmission by eqn. (2.2). On applying bias voltage due to potential difference of electrode, a kind of imbalance is created and current flows through the device and hence the transmission spectrum can be translated into current by eqn. (2.2). The I-V characteristics of device is displayed in Figure 4 within the range (0-2.5 V).
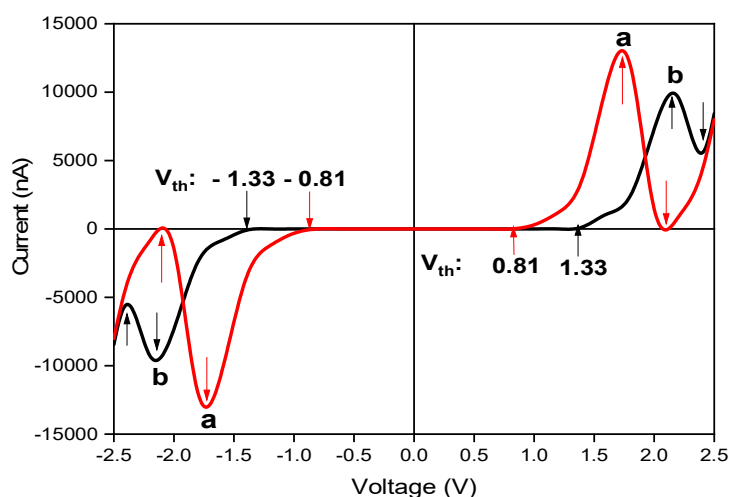
Figure 4. Calculated I-V characteristics of (a) 8-atoms long carbon chain based AGNR device (red solid line) and (b) 4-atoms long carbon chain based AGNR device (black solid line). Up (↑) and down (↓) shows the magnitude of current at peak and valley point of NDR respectively

The device remains inactive between 0 and 0.81 V, beyond 0.81 V, the current rises steeply. The threshold of the device is 0.81 V, beyond 0.81 V and upto 2.07 V, there is a non-linear region and displays a very sharp N-type NDR pattern whose various parameters are listed below in Table 1.

Table 1. Distinctive electronic transport parameters of 8-atoms long monoatomic chain. The parameters are compared with a similar devicecomprises of 4-atom long monoatomic carbon chain

S. No.	Channel/Dimensions (nm)	Device Dimension (nm)	$V_{th}(V)$	$I_P(\mu A)$	$V_P(V)$	$I_V(\mu A)$	$V_V(V)$	PVR
1.	8-atoms/0.93	3.5	0.81	13.0	1.74	0.01	2.07	1301
2.	4-atoms/0.40	2.9	1.33	9.9	2.16	5.5	2.40	1.8

V_{th}: Threshold Voltage; I_P, I_V: Magnitude of maximum (peak) and minimum (valley) value of current at the applied voltage V_P and V_V of the NDR region; PVR: peak to valley ratio of current

A higher PVR (peak to valley ratio) enhances the possibility of this device for various electronic applications utilizing NDR. Comparison of results of the two type of chains shows that V_{th} of 8 atoms long carbon chain is smaller, peak value of current is higher and PVR is approximately 722 times higher than the 4-atoms long carbon chain. The result of the present work is compared with similar type of calculations with 4-carbon atom chain carried out by us before [1]. The PVR ratio of the device investigated is also much higher than for the PVR values of other bigger and complex devices reported earlier. Figure 5(a) and (b) shows the variation of PDOS of the three components of the device, where the high (appearance of merged sharp peaks close to fermi level) and low value (occurrence of merged peaks far away from fermi level) of current is observed.
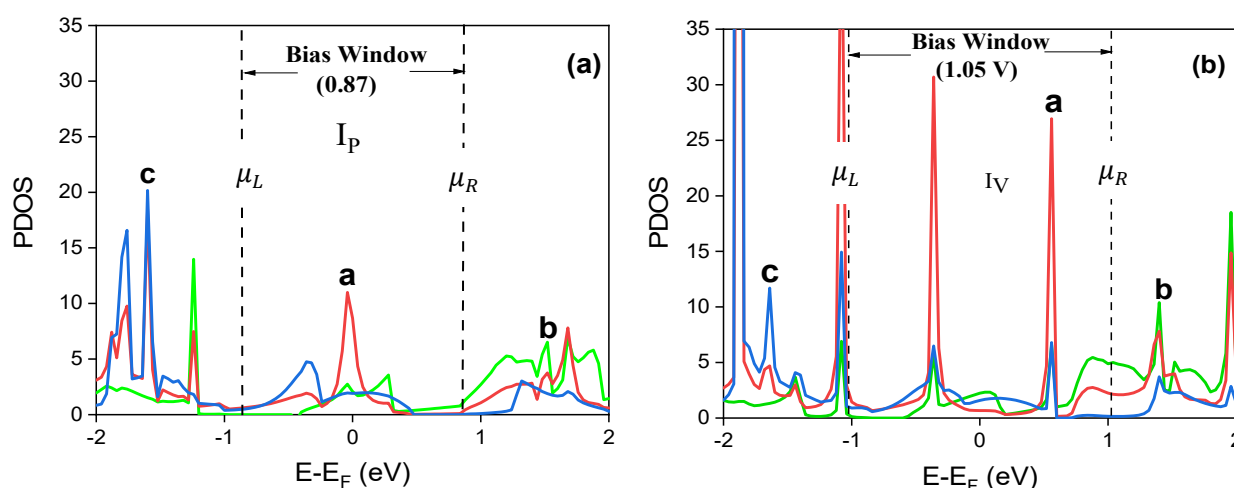
Figure 5. (a)Shows the partial density of states (PDOS) at voltage (0.86) where value of current is maximum (I_P) and (b) shows the PDOS at 1.06 V at the minimum value of current (I_V) of NDR region. Curve a, b, c depicts the PDOS of carbon chain, Left electrode and Right electrode respectively

The sharp merged peaks of PDOS at the fermi level (considered to be at 0 eV throughout this study) in Figure 5(a)at implies presence of finite no of available electronic states for efficient analyzation of charge carriers distributed within the proposed system of study. This further confirms strong correlation between the channel and the electrodes for hindrance free movement of electrons (implying ballistic transport) leading to instant rise in current value upto 13.0 μA (peak point) on surpassing the threshold voltage level 0.81. Similar trend is followed in Figure 5(b) which highlights the presence of lesser no of available density of states for electron transport due to merged PDOS peaks not being at fermi level leading to decrement in the current magnitude down to nearly zero level i.e. 0.01 μA (valley point). Further analysis of Figure 6(a) and (b) confirms the appearance of peak current 13.0 μA, with greater transmission magnitude area 0.14 a.u and valley current 0.01 μA, with negligible area 0.013 a.u with in the shaded red transmission region. Moreover, the high and low values of current can be attributed in terms of lowest unoccupied molecular orbital (LUMO) and highest occupied molecular orbital (HOMO) in molecular projected self consistent Hamiltonian (MPSH). In context to peak value of current, the LUMO (quantum number (QN) 199) are more delocalized over the transmission channel and extend upto electrodes implying enhancement in the no of valance electrons available for conduction. While, the HOMO (QN 200) tends to be localized over the bulk indicating lower concentration of valance electrons, thereby confirming the rise in current magnitude as depicted through Figure 6(c).

However, same pattern is followed for HOMO-LUMO for the case of valley point with a shift in delocalization of orbitals from LUMO to HOMO and localization from HOMO to LUMO as can be seen in Figure 6(d), which in turns give rise to lower current magnitude due to lesser concentration of valance electrons. Also, the corresponding red colour in MPSH indicates the respective region rich of electrons/ negative region suitable for electrophilic attack. While, the blue color represent the electron deficient/positive region favourable for nucleophilic intrusion. Hence, this forms the basis for NDR existence in the considered modeled device

which in turns enhance the possibility of such a device being implemented for various electronic applications such as logic design, fast triggering circuits, memory storage, high frequency oscillators [13, 24, 28, 37].
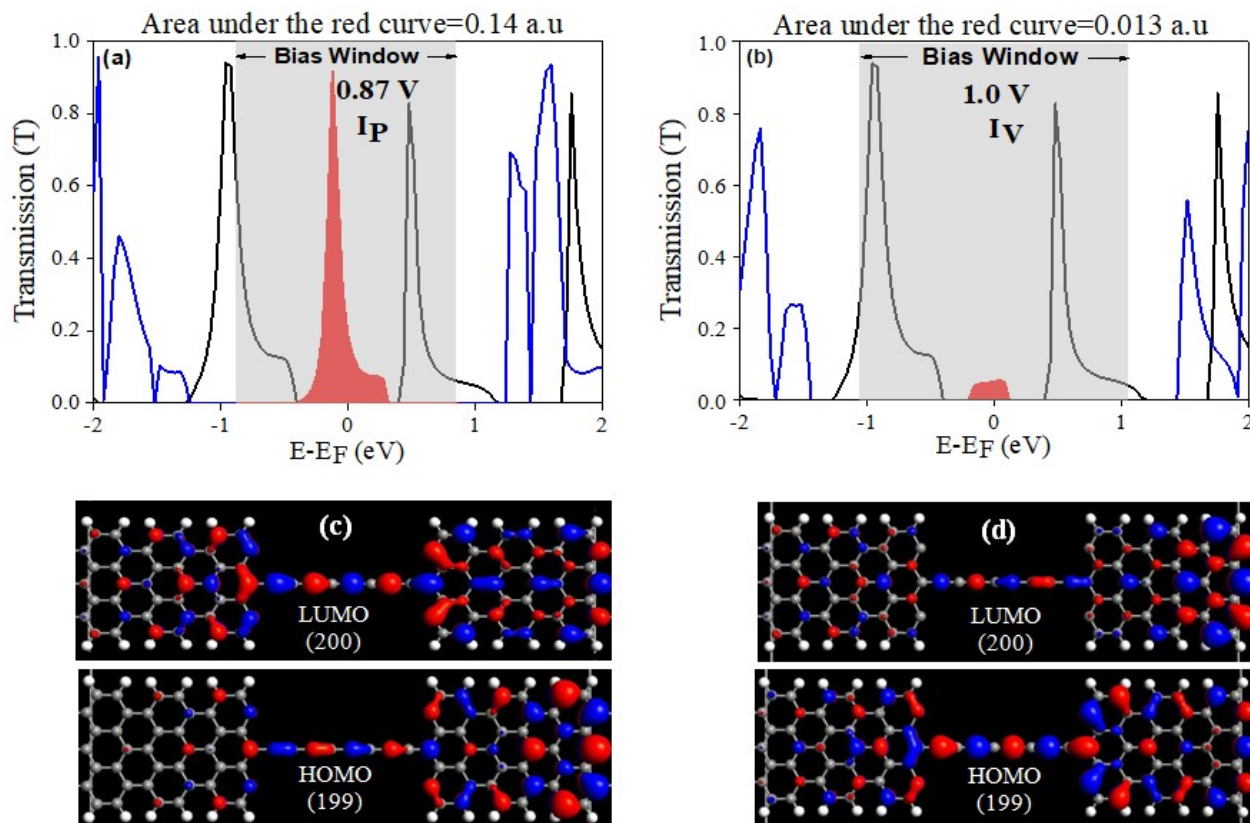

Figure 6. Transmission at maximum value of current $V = 0.87$ V (a) and minimum value of current $V = 1.00$ V, (b) The dark shaded area shows the magnitude of transmission within the bias window at these value of voltages as shown by grey shaded rectangle. MPSH (isovalue 0.05 a.u) is shown in (c) and (d) for maximum and minimum transmission

Besides, the appearance of NDR feature, there is also a remarkably astonishing feature incurred in the proposed device is its utilization as a simultaneous on and off switch corresponding to 2 V applied bias (as evident through I-V characteristic curve in Figure 4) by concurrently aligning the two form of device i.e. device with 4 carbon atom chain and 8-carbon atom chain as channel in a particular parallel fashion. This incurred feature in the considered device resembles the operation of a logic gate family member XOR gate, where in a simultaneous on and off operational input give rise to higher output. Based on this concept, the present device can act as an 2-input XOR gate with external input at left electrode (LE) as control enable input and thus paves way for realization of XOR logic gate operation at a particular voltage at nanoscale. Hence, the present device can be considered as a potential candidate in various field of nanoelectronics.

Further, we analyze the effect of *n*-type (Nitrogen doped)and *p*-type (Boron doped) doping of electrodes on the considered pristine carbon chain based nanodevice as shown in Figure 7(b)

and (a). It has been found out that although doping made the pristine device conducting by eliminating the nonconducting region as in pristine device shown in Figure 4. Instead, the doped device shows multiple NDR region with reduced PVR ratio to a maximum of 3.41 in the case of *p*-type case (Figure 7(a)), While attaining a maximum of 5.44 PVR ratio for *n*-type case (Figure 7(b)) which is much lower than the pristine device. This indicates that the effect of doping tends to degrade the overall PVR ratio besides enhancing the conductivity to several fold as shown in figure.
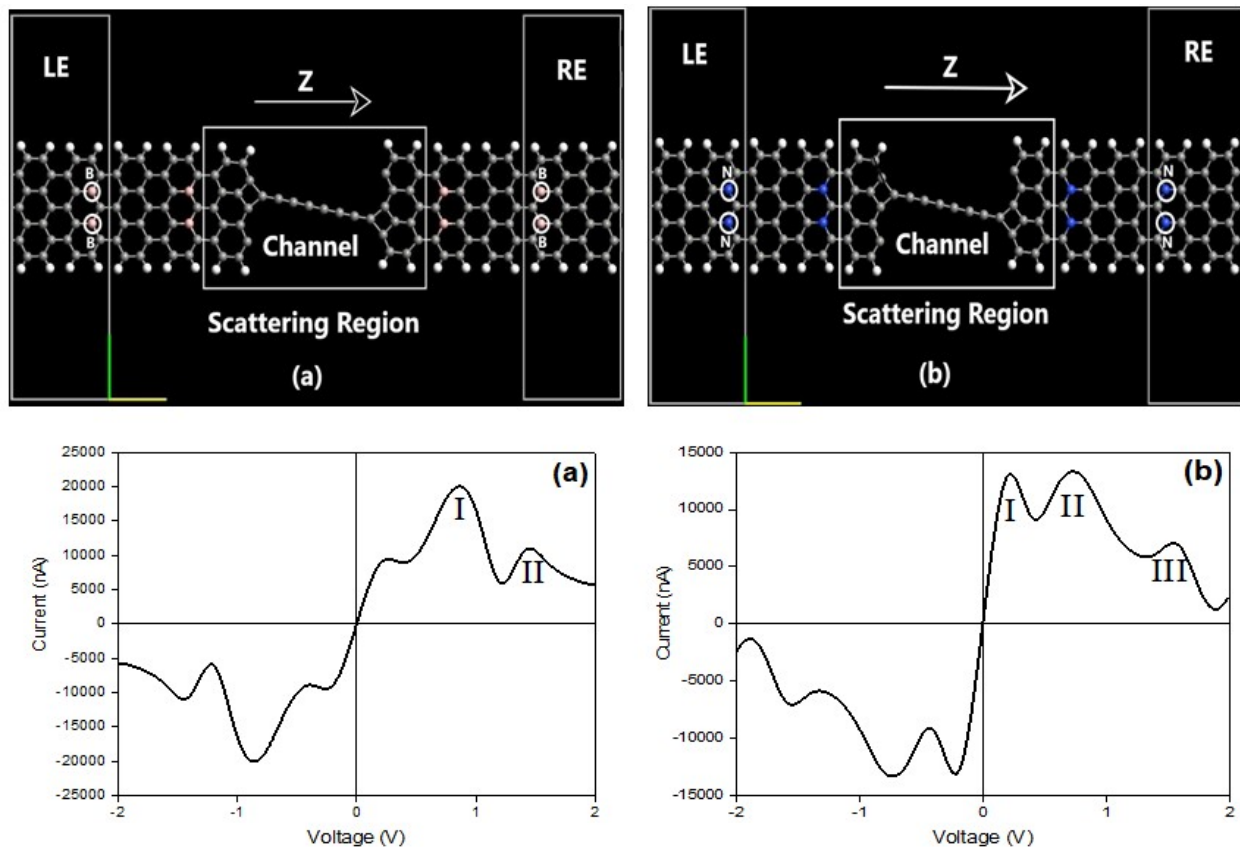

Figure 7. (a) Modeled structure and corresponding I-V curve of *p*-type doped device (b) N-type doped device, where I, II, III represents the successive NDR patterns

Hence, this has been in context to electron transport properties of proposed device that implies the present device be employed for multipurpose electronic applications, due to the unique characteristics exhibited by it.

4. Conclusion

Miniaturize device consisting of a 8-atom carbon monoatomic chain with 7-AGNR of size 3.5 nm is modeled and the electron transport is calculated by employing NEGF-DFT method resulting in a sharp NDR features. The I-V curve, at low voltage, resembles the characteristics similar to a semiconductor diode in forward bias and also that of an XOR logic gate (by simultaneous parallel implication of the present device with its successful replicant in a way of replacing the

existing channel (8-atom long carbon chain) with 4-atom long carbon chain). Additional features of NDR in the I-V characteristics of this carbon based device may be utilized to perform similar function as the conventional bulky and high power operating semiconductor diodes. The higher value of PVR (which is 1301) enhances its possibility for construction of application oriented electronic devices, as pointed out by previous workers working in the field.

Acknowledgment

We are thankful to the Department of Applied Sciences and Humanities, Jamia Millia Islamia for providing computational facilities**.**

Competing Interests

The authors declare that they have no competing interests.

Authors' Contributions

All the authors contributed significantly in writing this article. The authors read and approved the final manuscript.

References

[1] M. T. Ansari, M. M. Husain and M. Rafat, Modeling of carbon chain device employing quantum mechanical method: a hybrid diode, in *2018 IEEE Electron Devices Kolkata Conference* (EDKCON) 2018, November 24 (pp. 1 – 7), DOI: 10.1109/EDKCON.2018.8770516.

[2] M. Büttiker, Four-terminal phase-coherent conductance, *Physical Review Letters* **57** (1986), 1761, DOI: 10.1103/PhysRevLett.57.1761.

[3] D. W. Brenner, Empirical potential for hydrocarbons for use in simulating the chemical vapor deposition of diamond films, *Physical Review B* **42** (1990), 9458 – 9471, DOI: 10.1103/PhysRevB.42.9458.

[4] A. D. Carlo, M. Gheorghe, P. Lugi, M. Sternberg, G. Seifert and T. Frauenheim, Theoretical tools for transport in molecular nanostructures, *Physica B: Condensed Matter* **314** (2002), 86 – 90, DOI: 10.1016/S0921-4526(01)01445-4.

[5] L. Chen, L. He, H. S. Wang, H. Wang, S. Tang, C. Cong, H. Xie, L. Li, H. Xia, T. Li, T. Wu, D. Zhang, L. Deng, T. Yu, X. Xie and M. Jiang, Oriented graphene nanoribbons embedded in hexagonal boron nitride trenches, *Nature Communications* **8** (2017), 14703, DOI: 10.1038/ncomms14703.

[6] Ž. Crljen and G. Baranović, Unusual conductance of polyyne-nased molecular wires, *Physical Review Letters* **98** (2007), 116801, DOI: 10.1103/PhysRevLett.98.116801.

[7] S. Datta, *Quantum Transport: Atom to Transistor*, Cambridge University Press (2005), DOI: 10.1017/CBO9781139164313.

[8] S. Datta, Nanoscale device modeling: the Green's function method, *Superlattices and Microstructures* **28** (2000), 253 – 278, DOI: 10.1006/spmi.2000.0920.

[9] R. Denk, M. Hohage, P. Zeppenfeld, J. Cai, C. A. Pignedoli, H. Sode, R. Fasel, X. Feng, K. Müllen, S. Wang, D. Prezzi, A. Ferretti, A. Ruini, E. Molinari and P. Ruffieux, Exciton-dominated optical response of ultra-narrow graphene nanoribbons, *Nature Communications* **5** (2014) 4253, DOI: 10.1038/ncomms5253.

[10] V. Derycke, P. Soukiassian, A. Mayne, G. Dujardin and J. Gautie, Carbon atomic chain formation on the β-SiC(100) surface by controlled sp→sp3 transformation, *Physical Review Letters* **81** (1998), 5868 – 5871, DOI: 10.1103/physrevlett.81.5868.

[11] Y. J. Dong, X. F. Wang, M. X. Zhai, J. C. Wu, L. Zhou, Q. Han, X. M. Wu, Effects of geometry and symmetry on electron transport through graphene-carbon-chain junctions, *The Journal of Physical Chemistry C* **117** (2013), 18845 – 18850, DOI: 10.1021/jp405318b.

[12] M. Elstner, D. Porezag, G. Jungnickel, J. Elsner, M. Haugk, T. Frauenheim, S. Suhai and G. Seifert, Self-consistent-charge density-functional tight-binding method for simulations of complex materials properties, *Physical Review B* **58** (1998), 7260 – 7268, DOI: 10.1103/PhysRevB.58.7260.

[13] L. Esaki, New phenomenon in narrow germanium *p*-*n* junctions, *Physical Review* **109** (1958), 603, DOI: 10.1103/PhysRev.109.603.

[14] J. J. He, X. H. Yan, Y. D. Guo, C. S. Liu, Y. Xiao, L. Meng, The electron transport properties of zigzag grapheme nanoribbon with upright standing linear carbon chains, *Solid State Communications* **227** (2016), 28 – 32, DOI: 10.1016/j.ssc.2015.11.013.

[15] J. R. Heath, Q. Zhang, S. C. O'Brien, R. F. Curl, H. W. Kroto and R. E. Smalley, The formation of long carbon chain molecules during laser vaporization of graphite, *Journal of the American Chemical Society* **109** (1987), 359 – 363, DOI: 10.1021/ja00236a012.

[16] H. Huag and A. P. Jauho, *Quantum Kinetics in Transport and Optics of Semiconductors*, Springer Verlag (2008), DOI: 10.1007/978-3-540-73564-9.

[17] M. M. Husain and M. Kumar, Negative differential resistance, rectifying performance and switching behaviour in carbon chain based molecular devices, *Organic Electronics* **27** (2015), 92 – 100, DOI: 10.1016/j.orgel.2015.09.014.

[18] C. Jin, L. Haiping, P. Lianmao, S. Kazu, S. Iijima, Deriving carbon atomic chains from graphene, *Physical Review Letters* **102** (2009), 205501, DOI: 10.1103/PhysRevLett.102.205501.

[19] A. Kimouche, M. M. Ervasti, R. Drost, S. Halonen, A. Harju, P. M. Joensuu, J. Sainio and P. Liljeroth, Ultra-narrow metallic armchair graphene nanoribbons, *Nature Communications* **6** (2015), 10177, DOI: 10.1038/ncomms10177.

[20] S. Kotrechko, A. Timoshevskii, E. Kolyvoshko, Y. Matviychuk and N. Stetsenko, Thermomechanical stability of carbyne based nanodevices, *Nanoscale Research Letters* **12** (2017), 327, DOI: 10.1186/s11671-017-2099-4.

[21] R. Landauer, Philos, Electrical resistance of disordered one-dimensional lattices, *The Philosophical Magazine: A Journal of Theoretical Experimental and Applied Physics* **21** (1970), 863 – 867, DOI: 10.1080/14786437008238472.

[22] N. D. Lang and Ph. Avouris, Oscillatory conductance of carbon-atom wires, *Physical Review Letters* **81** (1998), 3515 – 3518, DOI: 10.1103/PhysRevLett.81.3515.

[23] J. P. Llinas, A. Fairbrother, G. B. Barin, W. Shi, K. Lee, S. Wu, B. Y. Choi, R. Braganza, J. Lear, N. Kau, W. Choi, C. Chen, Z. Pedramrazi, T. Dumslaff, A. Narita, X. Feng, K. Müllen, F. Fischer, A. Zettl, P. Ruffieux, E. Yablonovitch, M. Crommie, R. Fasel and J. Bokor, Short-channel field-effect transistors with 9-atom and 13-atom wide graphene nanoribbons, *Nature Communications* **8** (2017), 633, DOI: 10.1038/s41467-017-00734-x.

[24] H. Mizuta and T. Tanoue, *The Physics and Applications of Resonant Tunneling Diodes*, Cambridge University Press (2010), DOI: 10.1017/CBO9780511629013.

[25] S. Okano and D. Tománek, Effect of electron and hole doping on the structure of C, Si, and S nanowires, *Physical Review B* **75** (2007), 195409, DOI: 10.1103/PhysRevB.75.195409.

[26] D. Porezag, T. Frauenheim, T. Kohler, G. Seifert, R. Kaschner, Construction of tight-binding-like potentials on the basis of density-functional theory: application to carbon, *Physical Review B* **51** (1995), 12947 – 12957, DOI: 10.1103/PhysRevB.51.12947.

[27] Quantumwise a/s, *Atomistix Toolkit Version 12.2.2*, http://www.quantumwise.com.

[28] H. Ren, Q. X. Li, Y. Luo and J. L. Yang, Graphene nanoribbon as a negative differential resistance device, *Applied Physics Letters* **94** (2009), 173110, DOI: 10.1063/1.3126451.

[29] L. Talirz, P. Ruffieux and R. Fasel, On-surface synthesis of atomically precise graphene nanoribbons, *Advanced Materials* **28** (2016), 6222 – 6231, DOI: 10.1002/adma.201505738.

[30] S. Tongay, R. T. Senger, S. Dag and S. Ciraci, *Ab-initio* electron transport calculations of carbon based string structures, *Physical Review Letters* **93** (2004), 136404, DOI: 10.1103/PhysRevLett.93.136404.

[31] H. E. Troiani, M. M. Yoshida, G. A. C. Bragado, M. A. L. Marques, A. Rubio, J. A. Ascencio and M. J. Yacaman, Direct observation of the mechanical properties of single-walled carbon nanotubes and their junctions at the atomic level, *Nano Letters* **3** (2003), 751 – 755, DOI: 10.1021/nl0341640.

[32] N. Troullier and J. Martins, Efficient pseudopotentials for plane-wave calculations, *Physical Review B* **43** (1993), 1993 – 2006, DOI: 10.1103/PhysRevB.43.1993.

[33] T. H. Vo, M. Shekhirev, D. A. Kunkel, M. D. Morton, E. Berglund, L. Kong, P. M. Wilson, P. A. Dowben, A. Enders and A. Sinitskii, Large-scale solution synthesis of narrow graphene nanoribbons, *Nature Communications* **5** (2014), 3189, DOI: 10.1038/ncomms4189.

[34] Y. Xu, B. Wang, S. Ke, W. Yang, A. Z. Alzahrani, Highly tunable spin-dependent electron transport through carbon atomic chains connecting two zigzag graphene nanoribbons, *The Journal of Chemical Physics* **137** (2012), 104107, DOI: 10.1063/1.4752197.

[35] X. F. Yang, Z. G. Shao, H. L. Yu, Y. J. Dong, Y. W. Kuang and Y. S. Liu, Carbon chain-based spintronics devices: Tunable single-spin Seeback effect, negative differential resistance and giant rectification effects, *Organic Electronics* **55** (2018), 170 – 176, DOI: 10.1016/j.orgel.2018.01.023.

[36] Z. Zanolli, G. Onida and J. C. Charlier, Quantum spin transport in carbon chains, *ACS Nano* **4** (2010), 5174 – 5180, DOI: 10.1021/nn100712q.

[37] X. J. Zhang, M. Q. Long, K. Q. Chen, Electronic transport properties in doped C_{60} molecular devices, *Applied Physics Letters* **94** (2009), 073503, DOI: 10.1063/1.3082085.

[38] G. P. Zhang, X. W. Fang, Y. X. Yao, C. Z. Wang, Z. J. Ding and K. M. Ho, Electronic structure and transport of a carbon chain between graphene nanoribbon leads, *Journal of Physics: Condensed Matter* **23** (2011), 025302, DOI: 10.1088/0953-8984/23/2/025302.

[39] J. J. Zhang, Z. H. Zhang, J. Li, D. Wang, Z. Zhu, G. P. Tang, X. Q. Deng and Z. Q. Fan, Enhanced half-metallicity in carbon-chain-linked trigonal graphene, *Organic Electronics* **15** (2014), 65 – 70, DOI: 10.1016/j.orgel.2013.10.022.

[40] X. Zhao, Y. Ando, Y. Liu, M. Jinno and T. Suzuki, Carbon nanowire made of a long linear carbon chain inserted inside a multiwalled carbon nanotube, *Physical Review Letters* **90** (2003), 187401, DOI: 10.1103/physrevlett.90.187401.